LOW VELOCITY IMPACT RESPONSES AND IMPACT-INDUCED DAMAGES ON STEEL CORD-RUBBER COMPOSITE

N. Eiamnipon[1, 2*], P. Nimdum[1], J. Renard[1], C. Kolitawong[2]

[1]*Centre des Matériaux, Mines-ParisTech, CNRS UMR 7633, BP 87, 91003 Evry Cedex, France*
[2]*Department of Mechanical and Aerospace Engineering, King Mongkut's University of Technology North Bangkok, 1518 Pibulsongkram Road, Bangsue, 10800 Bangkok, Thailand*
**naruepon.eiamnipon@mines-paristech.fr*

Keywords: impact responses, impact damages, steel cord-rubber composite

Abstract
Steel cord-rubber composite lamina subjected to low velocity impact was investigated by a drop-weight method with a flat-ended impactor. This paper presents impact responses at different impact energy levels until failure. Energy based approach was used to analyze impact responses. Also impact-induced damages were observed by an optical camera. It revealed various modes of damages on the steel cord-rubber composite with increasing impact energy level.

1 Introduction

One of the major concerns in composite structures and designs is dynamic characterization in particular low velocity impact responses. Over two last decades, most research efforts have experimentally investigated on the impact responses, impact-induced damages and damage tolerance. It is due to much more uses of composite components in aeronautics and automobiles to gain high crashworthiness. Various high performance composite structures for example GFRP, CFRP, Graphite/PEEK were studied in many aspects such as different impact energy levels, specimen thickness, stacking sequences, clamping area, impactor shapes, preloads and etc [1-7].

However, another kind of composite structures recalled flexible composite such as steel cord-rubber composite has not sufficiently studied yet under low-velocity impacts. The experimental investigations on the steel cord-rubber composite were rarely reported in quasi-static tensile behavior with various cord orientations [8-10]. For high strain rate behavior and damage mechanisms, the steel cord-rubber composite were unveiled in these works [9-10].

The aim of this paper is to present low velocity impact responses on steel cord-rubber composite lamina using drop-weight impact method. It shows force-deflection diagrams and energy-time histories at different impact energy levels. Moreover, impact-induced damages and failure based on damage observation are investigated. Damage modes under low velocity impacts are to be described as impact energy level increases.

2 Material and testing equipments

2.1 Steel cord-rubber composite lamina

Steel cord-rubber composite is comprised of rubber reinforced with an array of steel cords. In this study, the steel cord-rubber composite was fabricated as unidirectional plate with low

steel cord volume fraction (18%). The diameter of the steel cord is approximately of 1.29 mm, which is formed by twisting small steel wires. The average thickness and the cord spacing are 2.67 and 2.72 mm respectively.

2.2 Impact testing

A drop-weight impact testing machine was developed at the Centre des Matériaux as demonstrated in Figure 1. It was used to carry out low velocity impact tests on the steel cord-rubber composite. The drop-weight impact machine consists of three main parts namely foundation, guiding column and cross-head impactor. The guiding column was fixed at the foundation whereas the cross-head impactor was able to slide freely on the guiding column. The maximum height of guiding column is 2.5 m. The impactor mass can be adjusted however it was fixed at 5 kg in this study. The flat tub with 6 mm in diameter was used in experiments. The Kistler 9071A load cell was mounted on the impactor in order to measure impact force during impact duration. The high speed digital camera was employed to record the displacement of the cross-head impactor with the capture speed of 10,000 images/s. The optical sensor attached to the cross-head impactor allowed synchronizing data acquisition between impact force and displacement of the impactor. A mechanical anti-rebound system was designed to protect one more impacts on the specimen. The cross-head impactor would be stopped on the guiding column by a locking pin while rebounding. In case of perforation, shock absorbers would absorb impact energy to protect the structure of the impact testing machine.

Due to high flexibility of the steel cord-rubber composite specimen, a clamping fixture had to be elaborately designed to eliminate a slippage during impact duration. In this study, the specimen was clamped on this fixture with a square impact area of 120x120 mm². Four different impact energy levels were conducted by varying impact height from 0.1 to 0.6 m, which corresponded to the impact energy levels of 4.4, 7.2, 13.7 and 28.7 J. Three to five specimens were used to study the low velocity impact tests each impact energy level.

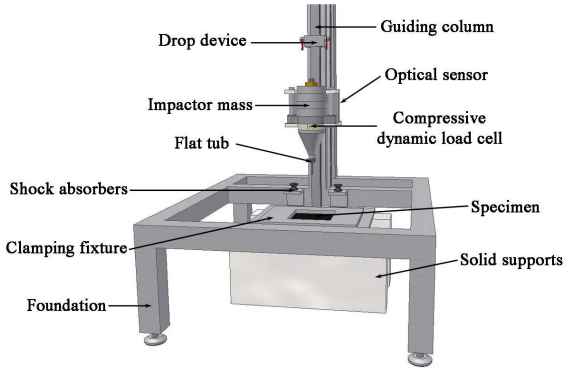

Figure 1. Schematic diagram of drop-weight impact testing machine.

3 Results and discussion

3.1 Experimental analysis

In order to analyze the low velocity impact responses such as force-deflection diagrams and energy-time histories, it should assume that the impactor was perfectly rigid and change in kinetic energy of the impactor was transformed to work done on the specimen or absorbed energy. The absorbed energy could be found in forms of damages on the specimen and heat dissipation. In these experiments, energy-time histories can be obtained by two approaches. One calculated a derivative of deflection-time histories $s_i(t)$ of the impactor recorded by the high speed digital camera as shown in equation (1):

$$v_i(t) = \frac{ds_i(t)}{dt} \tag{1}$$

where $v_i(t)$ is the velocity of the impactor during impact duration.
Another was an integration of force-time histories $F_{ext}(t)$ measured by the compressive dynamic load cell in equation (2):

$$v_i(t) = v_0 - \frac{1}{m}\int_0^t F_{ext}(t)dt \tag{2}$$

where v_0 and m are the initial velocity and the mass of the impactor respectively.
The kinetic energy can be expressed by the equation (3) and then the impact energy level is represented as the first term of the equation (3).

$$KE(t) = \frac{m}{2}\left(v_0^2 - v_i^2(t)\right) \tag{3}$$

Change in kinetic energy of the impactor is transformed to the work on the specimen as shown in equation (4) that can be also divided into absorbed energy by the specimen E_a and elastic energy due to rebound E_e.

$$KE(t) = \int_0^t F_{ext}(t).v_i(t)dt + loss = E_a + E_e \tag{4}$$

As we consider the equation (3) while replacing $v_i(t)$ from equation (1) we obtained change in kinetic energy of the impactor. Likewise, we are able to determine energy-time histories by means of an integration of the area under force-displacement diagrams in the equation (4). The difference in two approaches allows us obtain loss in transferring energy during impact event.

3.2 Impact responses
3.2.1 Force-deflection diagrams
Figure 2 shows force-deflection curves on the steel cord-rubber composite regarding four different impact energy levels (4.4, 7.2, 13.7 and 28.7 J). Impact responses under force-deflection diagrams presented three interesting regions according to deflection on the specimen. In the first region, deflection increased from the referent point to 3 mm the impact force remained nearly zero. This region resulted from a realignment of steel cords in the specimen. It was independent of the initial impact velocity or impact energy level. After the first region, force-deflection diagrams were in loading path up to the peak force. It showed that impact energy levels had strongly effects on the impact force and maximum deflection of the specimen. The impact force and maximum deflection increased with the impact energy level. The slope of force-deflection diagrams became a little bit stiffer when impact energy level increased. The final region was rebounding path after the maximum deflection. It displayed a reduction in impact force and residual deflections. The residual deflections were found that they went deeper with increasing the impact energy level.
Area under closed curves of force-deflection diagrams represented absorbed energy by the specimen. In case of perforation, there was no rebounding path. The impact force reduced immediately to zero at the maximum deflection because the specimen no longer underwent

impact force. At this peak force, it can be considered as impact force resistance of the steel cord-rubber composite.

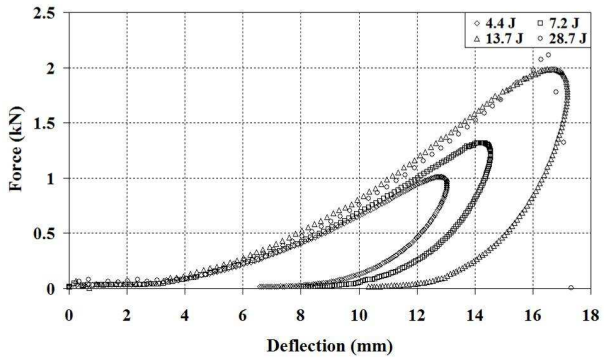

Figure 2. Force-Deflection diagrams for different impact energy levels.

3.2.2 Energy-time histories

As we consider the equation (4) loss in transferring energy was less than 5 % in these experiments, comparing overall energy-time histories. This loss was dissipated into other forms such as friction between impactor and specimen, viscous damping in the rubber, vibration of the specimen during impact event or heat dissipation. However, loss due to transferring energy between kinetic energy and work done on specimen can be neglected. Based on the energy approach, Figure 3 demonstrated two energy parts: absorbed energy E_a at the end of energy-time histories and elastic energy E_e corresponding to the difference in two energy values between the maximum energy point and the absorbed energy. The elastic energy can be considered as rebounding energy. The maximum energy points in energy-time histories coincided with the impact energy levels.

According to energy-time histories, we found that absorbed energy and elastic energy tended to increase with the impact energy level. For the highest impact energy level of 28.7 J, the energy transferring from the impactor became absorbed energy by the specimen without elastic energy. It was due to a perforation on the specimen. However, the absorbed energy was not the whole impact energy level. The kinetic energy of the impactor still remained after the perforation on the specimen. At the perforation, the absorbed energy was considered as impact absorbed energy resistance of the steel cord-rubber composite.

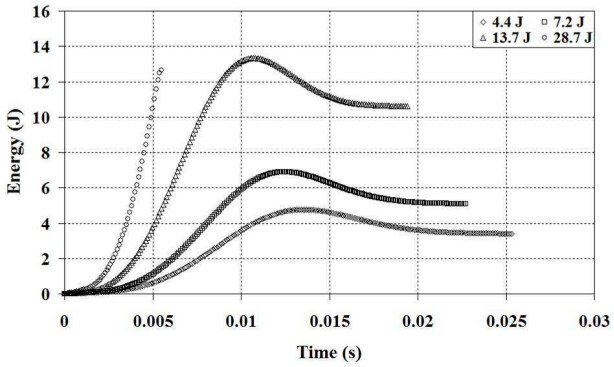

Figure 3. Energy-Time histories for different impact energy levels.

3.3 Impact-induced damages and failure

A damage observation under low velocity impact tests was conducted by an optical camera. In this observation, several kinds of damages were identified. The specimens were thoroughly investigated at the front face and back face after the impact tests.

The damages induced by flat tub on the steel cord-rubber composite lamina can be categorized with the impact energy levels. At low impact energy levels of 4.4 and 7.2 J, compressive damage on rubber existed on the front face. A circular trace appeared due to the shape of the flat tub. The back face had no damage existence. With increasing impact energy level, the circular trace became more explicit. At impact energy level of 13.7 J, the impact-induced damages exhibited evidently as long rubber cracks parallel to the steel cord. These cracks were generated by the flat tub and then propagated along the circular trace. The residual deflection was due to warping of the steel cord subjected to the flat tub. At the highest impact energy level of 28.7 J, the specimen failed under steel cord breakage. The perforation occurred throughout from front face to back face. The short rubber cracks parallel to the steel cords were also observed at the perforated hole.

4 Conclusions

Steel cord-rubber composite subjected to low velocity impact was investigated under drop-weight impact tests. Impact responses were presented as force-deflection diagrams and energy-time histories. They revealed dynamic characteristics of the steel cord-rubber composite lamina with increasing impact energy level. Also impact-induced damages were observed after impact tests. Three kinds of damages were unveiled: compressive damage on the rubber front face at low impact energy level, rubber cracking parallel to the steel cord at nearly critical impact energy level and steel cord breakage at high impact energy level. A perforation was caused of steel cord breakage in the specimen.

This study leads us to profoundly understand impact responses and impact-induced damages of the steel cord-rubber composite subjected to low velocity impact. These dynamic characteristics have to be paid attention for a design of cord composite structures.

Acknowledgements

The authors would like to express sincerely our gratitude to the Royal Golden Jubilee Ph.D. Program (IUG50K0008), Michelin Research Asia and French Embassy for their financial support in this work. We also thank Centre de Technologie de Ladoux, Michelin France especially Mr. Eric Carin Neba and Mr. Jean Coé for supplying materials. We also wish to thank Dr. Banpot Horbanluekit and Mr. Marc Auriacombe for their helpful comments.

References

[1] Belingardi G., Vadori R. Low velocity impact tests of laminate glass-fiber-epoxy matrix composite material plates. *International Journal of Impact Engineering*, **27**, pp. 213-229 (2002).

[2] Sutherland L.S., Guedes Soares C. Impact characterisation of low fibre-volume glass reinforced polyester circular laminated plates. *International Journal of Impact Engineering*, **31**, pp. 1-23 (2005).

[3] Mitrevski T., Marshall I.H., Thomson R. The influence of impactor shape on the damage to composite laminates. *Composite Structures*, **76**, pp. 116-122 (2006).

[4] Robb M.D., Arnold W.S., Marshall I.H. The damage tolerance of GRP laminates under biaxial prestress. *Composite Structures*, **32**, pp. 141-149 (1995).

[5] Aymerich F., Bucchioni A., Priolo P. Impact behaviour of quasi-isotropic graphite-peek laminates. *Key Engineering Materials*, **144**, pp. 63-74 (1998).

[6] Tita V., de Carvalho J., Vandepitte D. Failure analysis of low velocity impact on thin composite laminates: Experimental and numerical approaches. *Composite Structures*, **83**, pp. 413-428 (2008).

[7] Liu D., Raju B.B., Dang X. Impact perforation resistance of laminated and assembled composite plates. *International Journal of Impact Engineering*, **24**, pp. 733-746 (2000).

[8] Cembrola R.J., Dudek T.J. Cord/rubber material properties. *Rubber Chemistry and Technology*, **58**, pp. 830-856 (1985).
[9] Rao S., Daniel I.M., Gdoutos E.E. Mechanical properties and failure behaviour of cord/rubber composites. *Applied Composite Materials*, **11**, pp. 353-375 (2004).
[10] Eiamnipon N., Nimdum P., Renard J., Kolitawong C., Horbanluekit B., Auriacombe M. High strain rate behavior of steel cord rubber composite for pneumatic tyre in "Proceeding of the 12th Japanese-European Symposium on Composite Materials", Jeju island, Korea, (2011).